 Bull. Chem. Soc. Jpn. Vol. 81, No. 9, 1175–1182 (2008)

Effects of Added CO_2 and H_2 on the Direct Decomposition of NO over $BaMnO_3$-Based Perovskite Oxide

Hideharu Iwakuni, Yusuke Shinmyou, Hiroaki Yano, Kazuya Goto, Hiroshige Matsumoto, and Tatsumi Ishihara*

Department of Applied Chemistry, Faculty of Engineering, Kyushu University, 744 Motooka, Nishi-ku, Fukuoka 819-0395

Received January 24, 2008; E-mail: ishihara@cstf.kyushu-u.ac.jp

N_2 yield on $Ba_{0.8}La_{0.2}Mn_{0.8}Mg_{0.2}O_3$ decreased from 70% to 30% on the addition of 1% CO_2, which is a much larger negative effect than that seen with O_2. The CO_2 negative effects are not permanent and this may result from the inhibition of NO adsorption. Co-feeding of H_2 as a reductant is effective for increasing NO conversion. This suggests that the catalyst surface was covered with strongly adsorbed nitrate or nitride species which formed by adsorption of NO on oxygen formed by the decomposition of NO, and the removal of this surface species might be the most important step for the NO decomposition reaction. Co-feeding of H_2 is also effective for increasing the NO decomposition activity in the presence of CO_2. The reaction mechanism was studied by IR measurements which also revealed that the surface of the catalyst was covered with strongly bound nitrate species (NO_3^-). The addition of H_2 to the reaction mixture is effective for NO_3^- removal and so accelerates the NO decomposition under coexistence of CO_2.

At present, because of the increase in the number of diesel engine cars, the amount of NO emissions in urban areas has been increasing. Nitrogen oxides (NO_x) are extremely toxic to the human body and are also harmful to the environment as a principal source of both acid rain and photochemical smog. Several methods have been proposed for NO_x removal.[1–19] Among them, the selective reduction of NO_x with urea is now considered the most promising method for the removal of NO_x in an oxygen-containing atmosphere such as an exhaust gas from diesel engines. However, if unreacted urea or ammonia which forms from urea is released, there are also deleterious effects on environment. Direct decomposition of NO into N_2 and O_2 ($2NO = N_2 + O_2$) is the most ideal reaction to remove NO_x because the process is quite simple.[20,21] However, due to the strong adsorption of oxygen formed, NO decomposition activity of the conventional catalyst decreases under oxygen-containing atmosphere. Catalysts, such as Cu-ZSM-5,[22] Co-ZSM-5 (which contains Co in the framework[23]), La_2O_3,[24] Ba/MgO,[25] and $LaCoO_3$[26,27] based perovskite oxides, are reported to be active for the direct decomposition of NO. In addition to these reports, the catalysts with perovskite or perovskite-related structure, i.e., $La_{0.4}Sr_{0.6}Mn_{0.8}Ni_{0.2}O_3$[28] or $La_{0.7}Ce_{0.3}SrNiO_4$[29] are reported to be active to NO decomposition under oxygen-containing atmosphere. However, up to now, no catalyst exhibits high NO decomposition activity under realistic conditions. From the viewpoint of a practical application of this process, in some cases, increasing the reaction temperature is beneficial because the negative effects of oxygen, water, and sulfur compounds are expected to be reduced with increasing reaction temperature. Therefore, although the reaction condition is not close to realistic conditions, NO decomposition on perovskite oxide still has a possibility for NO removal in particular at high temperature.

In our previous study, $LaMnO_3$ perovskite oxide doped with Ba for the La site and In for the Mn site, which mainly consists of Mn^{III}, has been investigated and it was found that $La_{0.7}Ba_{0.3}Mn_{0.8}In_{0.2}O_3$ perovskite oxide exhibited a high activity for the direct decomposition of NO at temperatures higher than 1073 K.[30] On the other hand, it was found that $Ba_{0.8}La_{0.2}Mn_{0.8}Mg_{0.2}O_3$, which mainly consists of Mn^{IV} and Mn^{III} from the phase diagram, is highly active for the direct NO decomposition reaction.[31] Although the composition is similar, the catalysis of $Ba_{0.8}La_{0.2}Mn_{0.8}Mg_{0.2}O_3$ is interesting because the catalyst contains Mn^{4+} species, which is an anomalous valence of Mn at temperatures higher than 773 K and redox of Mn would be expected to occur easily. Both catalysts show rather high activity under oxygen co-feeding and comparing with that of $La_{0.7}Ba_{0.3}Mn_{0.8}In_{0.2}O_3$ catalyst, N_2 yield on $Ba_{0.8}La_{0.2}Mn_{0.8}Mg_{0.2}O_3$ is slightly higher. On this catalyst, N_2 and O_2 formation is observed above 873 K and yield of N_2 and O_2 are 75% and 60%, respectively at 1123 K. Comparing the activity for NO decomposition of the conventional perovskite oxide, activity of this $Ba_{0.8}La_{0.2}Mn_{0.8}Mg_{0.2}O_3$ oxide is encouragingly high. The reasonably high N_2 yield on this catalyst is also sustained in the presence of O_2[31] (38% at 1123 K, 5% O_2, which is slightly higher than those of the perovskite-related oxide of $La_{0.7}Ce_{0.3}SrNiO_4$ (32%)[29] and our previously reported $La_{0.7}Ba_{0.3}Mn_{0.8}In_{0.2}O_3$ (15%),[30] although the reaction conditions are slightly different). In the present study, effects of co-feeding CO_2 and H_2 on NO decomposition activity on this $Ba_{0.8}La_{0.2}Mn_{0.8}Mg_{0.2}O_3$ were investigated. In addition, the mechanism of these co-feeding gases on NO decomposition was studied with temperature-programmed desorption (TPD) and IR absorption methods.

Published on the web September 11, 2008; doi:10.1246/bcsj.81.1175

Experimental

Doped $BaMnO_3$ was prepared by a conventional solid-state reaction method of which details are described in our previous report.[31] It is noted that the formation of the perovskite phase of $BaMnO_3$ was confirmed by XRD.[31] BET surface area of the obtained $Ba_{0.8}La_{0.2}Mn_{0.8}Mg_{0.2}O_3$ catalyst is as small as $1.3\,m^2\,g^{-1}$.

The direct decomposition of NO was performed with a conventional fixed-bed gas-flow reactor with a quartz glass tube (12-mm diameter), which is the same as that of our previous study.[31] Here, it is noteworthy that the formation of NO_2 is observed by the reaction of NO and O_2 formed in NO decomposition and so the yield of N_2 is always higher than that of O_2. The activity of the catalyst for NO decomposition is discussed mainly in terms of the N_2 yield in this study. No N_2O formation is observed in this study.

The effects of adding CO_2 were measured in a range from 1–5 vol % which is obtained by mixing He with the commercial 21 vol % O_2 or 10% CO_2 diluting in He gases. In order to keep the total reactant flow rate of $20\,mL\,min^{-1}$ constant, we changed the feed rate of He as a balance gas. The effects of the addition of H_2 on the NO decomposition were also measured, using H_2 diluted to 1000 ppm with He mixed with 1000 ppm NO diluted with He.

For the NO and O_2 temperature-programmed desorption (TPD), after evacuation of the catalyst at 773 K for 1 h, the catalyst was exposed to 101.3 kPa NO or O_2 for 30 min at the same temperature, then cooled to room temperature. A CO_2 TPD measurement was also carried out by CO_2 adsorption at 101 kPa, 773 K for 30 min prior to the NO adsorption treatment at 773 K for 0.5 h. In the H_2 treatment case, the catalyst was exposed to H_2 at 101 kPa at 773 or 573 K after the O_2 adsorption treatment at 773 K for 0.5 h. In all cases, after having been cooled to room temperature with $100\,K\,min^{-1}$ in gas flow of the final adsorption treatment and evacuated at 323 K for 30 min, the catalyst was heated at $10\,K\,min^{-1}$, and the desorbed gas was monitored by a quadrupole mass spectrometer (ANELVA, AQR-100R).

The adsorption state of the NO on the catalyst was measured with FT-IR (JASCO type 610) using a diffusion reflectance measurement set-up. Since the color of $BaMnO_3$ catalyst studied is black, we used a HgCdTe semiconductor (MCT) detector, which is a sensitive IR detector and a diffuse reflectance system. About 100 mg of the catalyst powder was placed in an in situ measurement cell with KBr single-crystal windows. Before the measurement, the catalyst was evacuated at 773 K for more than 3 h, and then the background spectrum was measured at room temperature. After NO (ca. 10 kPa) was introduced, the catalyst was heated at 773 K for 30 min as the gas circulated.

Results and Discussion

Effect of CO_2 and H_2 on NO Decomposition over $Ba_{0.8}La_{0.2}Mn_{0.8}Mg_{0.2}O_3$. In order to investigate NO decomposition activity in further detail, we studied the effects of CO_2 coexistence on NO decomposition activity. CO_2 is one of the major components in exhaust gas and it is reported that CO_2 shows negative effects similar to O_2 existence.[27] Tofan et al. have reported[32] that inhibition of NO decomposition by CO_2 was quite significant over the three perovskite catalysts, i.e., $La_{0.87}Sr_{0.13}Mn_{0.2}Ni_{0.8}O_{3-\delta}$, $La_{0.66}Sr_{0.34}Ni_{0.3}Co_{0.7}O_{3-\delta}$, and $La_{0.8}Sr_{0.2}Cu_{0.15}Fe_{0.85}O_{3-\delta}$. Liu et al. have also reported that CO_2 inhibition over a $Ag/La_{0.6}Ce_{0.4}CoO_3$ catalyst is quite large, although it is reversible.[33] Hence, we anticipated that co-feeding CO_2 would have a large negative effect on the direct NO decomposition on $Ba_{0.8}La_{0.2}Mn_{0.8}Mg_{0.2}O_3$. Figure 1 shows the actual NO, N_2, and O_2 yields as a function of the CO_2 partial pressure at 1123 K. The N_2 yield decreased from 70% to 30% with the addition of 1% CO_2, a much larger negative effect than that of O_2. N_2 yield decreased from 30 to 18% in the P_{CO_2} range from 1% to 5%. As a result, even for a 5% CO_2 partial pressure, a N_2 yield of 20% was sustained. Figure 2 shows that the N_2 formation rate as a function of CO_2 partial pressure monotonically decreased with increasing P_{CO_2}, with a power P_{CO_2} dependency estimated to be -0.32. However, considering the high concentration of CO_2 in exhaust gas, the negative effects of CO_2 on NO decomposition are rather serious.

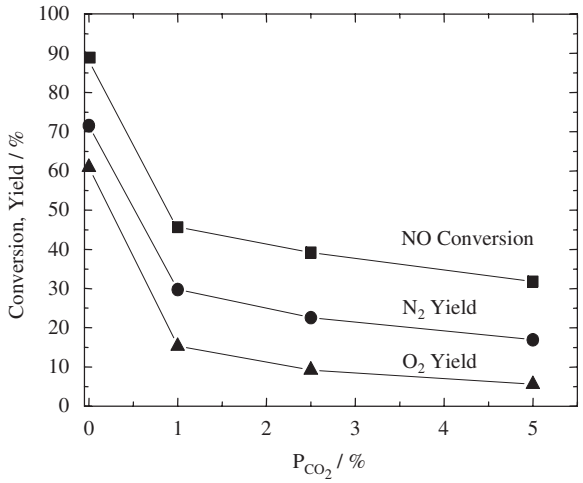

Figure 1. N_2 and O_2 yield as a function of CO_2 partial pressure over $Ba_{0.8}La_{0.2}Mn_{0.8}Mg_{0.2}O_3$ at 1123 K (P_{NO} = 1%, $W/F = 3.0\,g\,s\,cm^{-3}$).

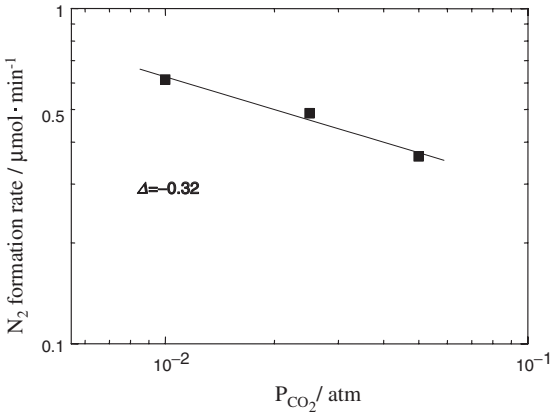

Figure 2. N_2 formation rate as a function of CO_2 partial pressure at 1223 K (P_{NO} = 1%, $W/F = 3.0\,g\,s\,cm^{-3}$).

Figure 3 shows the time dependence of the N_2 and O_2 yield after introduction, then cutting a 5% CO_2 co-feed for the reaction over $Ba_{0.8}La_{0.2}Mn_{0.8}Mg_{0.2}O_3$ at 1123 K. The formation rates of N_2 and O_2 decreased on co-feeding of CO_2 (as discussed earlier); however, it gradually recovered to the original formation rates a few hours after cutting the CO_2 co-feed.

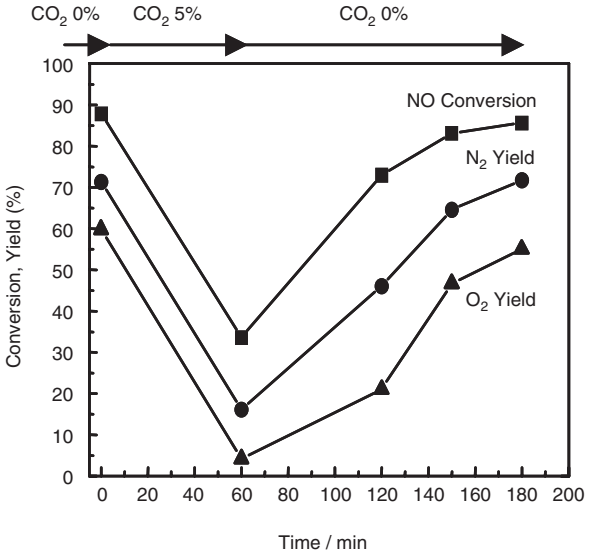

Figure 3. Time dependence of N_2 and O_2 yield after providing, then removing, a 5% CO_2 co-feed on NO decomposition over $Ba_{0.8}La_{0.2}Mn_{0.8}Mg_{0.2}O_3$ at 1123 K ($P_{NO} = 1\%$, $W/F = 3.0\,g\,s\,cm^{-3}$).

Therefore, it is obvious that the negative effects of CO_2 are not permanent and may result from the inhibition of NO adsorption by strong adsorption of CO_2 rather than the decomposition of the catalyst by the formation of carbonate. This is also confirmed by XRD measurements after reaction, namely, the perovskite structure of the $BaMnO_3$ is not changed after NO decomposition measurements with CO_2 added to the reactants.

In our previous study of the reaction mechanisms on the $LaMnO_3$-based perovskite oxide,[30] it is suggested that the surface of the catalyst is covered with nitrate species formed at low temperatures and the removal of these nitrate species requires a high temperature or a reductant. Therefore, the most significant drawback of NO decomposition on a perovskite oxide catalyst is the high reaction temperature needed to achieve high NO decomposition activity. However, if strongly adsorbed surface NO_x species could be removed, then the NO decomposition might proceed at intermediate temperatures around 773 K. In our previous study, the N_2 formation rate was drastically improved by the addition of H_2, producing a N_2 yield as high as 60% even at the low temperature of 773 K. This could be explained by the removal of the strongly adsorbed oxygen or the surface nitrate species with H_2, which is discussed further later, based on the TPD and IR results. On the other hand, negative effects of CO_2 co-feeding are similar effects of O_2 coexistence and so, addition of a small amount of reductant seems to be effective for improving N_2 yield even under CO_2 co-feeding atmosphere.

Since it was found that the addition of H_2 was effective for increasing the NO decomposition activity in our previous study,[30] the effects of H_2 in the presence of CO_2 were investigated in this study. Figure 4 shows the temperature dependence of the N_2 formation rate with the addition of H_2 and for an added mixture of H_2 and CO_2. In this experiment, we used 0.1% NO by experimental reasoning, however, the effects of NO partial pressure and H_2 co-feeding are reported in our previous study.[31] NO decomposition hardly occurred at temperatures lower than 673 K and even at 1123 K, N_2 yield is as small as 8% when CO_2 was added at 5%. Although the N_2 yield under a CO_2-containing atmosphere is smaller than that without CO_2, it can be seen that the N_2 yield was much improved by addition of H_2 even when CO_2 was present. The N_2 yield at 1123 K with added H_2 is almost the same (ca. 70%) with, or without CO_2. On the other hand, N_2 yield once decreased at 777 K under NO–H_2–CO_2 conditions. As will be discussed later, molecular adsorption of NO is dominant at lower temperature but dissociative at higher temperature. We speculate that adsorbed NO is directly reacted with H_2 at lower temperature but at high temperature, added hydrogen mainly reacted with the formed surface oxygen because of the high dissociation reaction rate of NO. Therefore, by changing the reaction step, NO decomposition is once decreased around 777 K. In any case, when reducing agents such as H_2 are employed, the negative effects of CO_2 seem to be mitigated. The real exhaust gas from internal combustion engines contains small amounts of reducing agents like CO or unburned fuel which may act to reduce the negative effects of CO_2 contained in the exhaust gas. Of course, the addition of H_2 as a reducing agent is not realistic for practical applications, however, positive effects of co-feeding H_2 suggests that the negative effects of CO_2 are produced by the strong adsorption of CO_2 on the active site for NO decomposition and this could be studied with further detailed adsorption measurements.

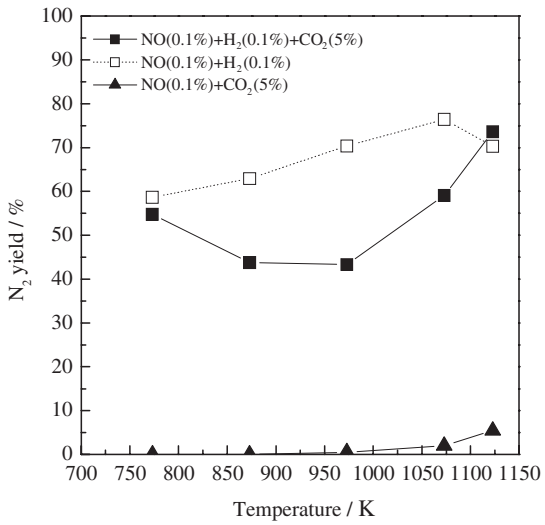

Figure 4. Temperature dependence of NO direct decomposition with added H_2 and CO_2 over $Ba_{0.8}La_{0.2}Mn_{0.8}Mg_{0.2}O_3$ ($P_{NO} = 1\%$, $W/F = 3.0\,g\,s\,cm^{-3}$).

Effects of H_2 on NO and O_2 Adsorption States. The effects of co-fed H_2 on the adsorption state of oxygen were studied by temperature-programmed desorption (TPD) and IR measurements. Figure 5 shows the O_2 desorption profiles from $Ba_{0.8}La_{0.2}Mn_{0.8}Mg_{0.2}O_3$ after exposure to H_2. On a catalyst that had not been exposed to hydrogen, a large O_2 desorption was observed at 773 K and a small shoulder exists between 973 and 1073 K. According to a report by Spinicci et al. on oxygen desorption from a Mn-based perovskite oxide, the oxygen desorbed above 1073 K could be assigned to the desorption of lattice oxygen, and that occurring below 973 K was assigned

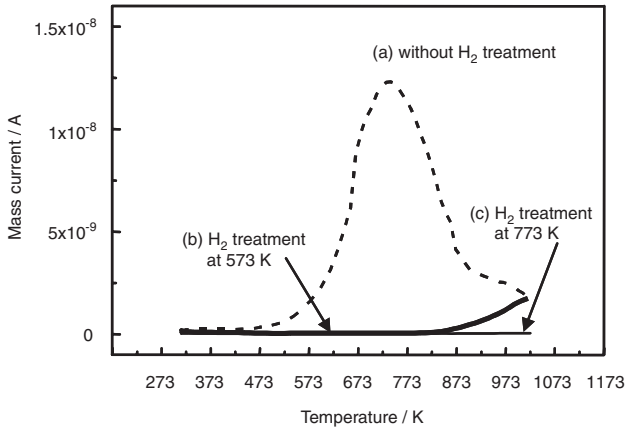

Figure 5. O_2-TPD profile of $Ba_{0.8}La_{0.2}Mn_{0.8}Mg_{0.2}O_3$ after exposure to H_2 at 573 and 773 K (O_2 adsorption: 773 K for 30 min; H_2 treatment: 573 or 773 K for 30 min after O_2 adsorption).

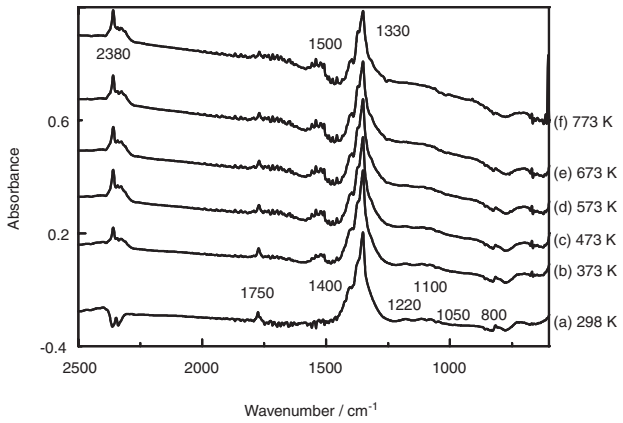

Figure 6. IR spectra of adsorbed NO on $Ba_{0.8}La_{0.2}Mn_{0.8}Mg_{0.2}O_3$ (NO adsorption: 773 K for 1 h).

to adsorbed oxygen.[34] Therefore, we assign the desorption observed in Figure 5a to adsorbed oxygen. Figures 5b and 5c also show O_2-TPD data on $Ba_{0.8}La_{0.2}Mn_{0.8}Mg_{0.2}O_3$ after exposure to H_2 at 573 and 773 K. As expected, the amount of desorbed oxygen drastically decreased; almost no oxygen desorption was observed after exposure to H_2 at 773 K, but a small amount of O_2 desorption was observed after treatment with H_2 at 573 K. This suggests that the strongly adsorbed surface oxygen can be easily removed by exposure to H_2 at 773 K. This is also the temperature at which large positive effects of H_2 addition was observed on NO decomposition. Therefore, it is reasonable to suggest that one reason for the positive effects of co-feeding hydrogen may come from the removal of strongly adsorbed surface oxygen or NO_x species.

Figure 6 shows the IR spectra of adsorbed NO on $Ba_{0.8}La_{0.2}Mn_{0.8}Mg_{0.2}O_3$ after adsorption at 773 K for 1 h. After evacuation of the gaseous NO, the spectrum at 298 K showed several absorption peaks around 2380, 1750, 1400, 1330, 1220, 1100, 1050, and 800 cm^{-1}. The peaks around 2380 cm^{-1} can be assigned to CO_2 in the spectrometer beam lines, since the measurement is performed in the single beam mode. According to the reported values,[35] the peaks around 1750, 1330, and 1220 cm^{-1} can be assigned to the bent type NO adsorption (NO^-), and the bridging and the monodentate nitrate species (NO_3^-), which could be either OO–NO^- or O–NOO^- species, respectively. After evacuation at 473 K, the absorption peak around 1750 cm^{-1} decreased. In NO TPD measurement, NO desorption occurs by NO, O_2, and N_2 and no N_2O or NO_2 desorption was observed.[31] In the low-temperature range, desorption of molecular NO is dominant. However, NO desorption cannot be observed at temperatures higher than 873 K. In contrast, O_2 and N_2 desorption is mainly observed at temperatures higher than 673 K, the temperature region in which the NO decomposition reaction starts to proceed. On the other hand, a small amount of N_2 desorption is observed at 473 K, the temperature region in which NO desorption occurs. However, no desorption of oxygen was observed at this lower temperature. Therefore, it is considered that both molecular and dissociative NO adsorption occurs on this catalyst and the weakly adsorbed molecular NO desorbed at a relatively low temperature. However, some part of the dissociatively adsorbed NO desorbed as N_2 around 873 K and the resulting oxygen remains on the surface as nitrate or nitrous species of NO_3^- or NO_2^-, respectively and block the active site for NO decomposition. The formation of NO_3^- or NO_2^- species is also observed on $LaMnO_3$ oxide.[30] Therefore, the absorption peak around 1750 cm^{-1} may correspond to the lower temperature NO desorption peak in NO-TPD. The absorbance of the peaks around 1400 and 800 cm^{-1} decreased gradually with increasing evacuation temperature. Therefore, NO desorption around 573 K in the NO-TPD could be assigned to desorption of these surface NO_x species.

On the other hand, the other peaks are rather strong and did not disappear after evacuation at 773 K. As discussed for the NO-TPD results, O_2 desorption followed by N_2 desorption was observed at temperatures higher than 773 K. In particular, one strong peak around 1330 cm^{-1}, which could be assigned to chelated nitrite (OO–N^-), is almost unchanged after the 773 K evacuation. Therefore, surface chelated nitrite species is very strongly adsorbed and is not easily removed. The desorption temperature data suggest that the surface of $BaMnO_3$ is covered with nitrate or nitrite (NO_2^-) species, which forms on the adsorption of NO on surface oxygen, at temperatures below those needed for the NO decomposition reaction and the removal of these species, namely recovery of the active site, is important for the NO decomposition reaction to proceed. In comparison with the other catalysts, such as $LaMnO_3$[30] or $LaCoO_3$,[27] the desorption temperatures of O_2 and N_2, i.e. the removal of surface adsorption species occurs at rather lower temperatures on the $Ba_{0.8}La_{0.2}Mn_{0.8}Mg_{0.2}O_3$ catalyst, resulting in the high NO decomposition activity.

The surface adsorption species present under conditions where the NO decomposition reaction takes place was further studied by IR measurements taken at 973 and 1073 K and the results are shown in Figure 7. A number of absorption peaks were observed, some of them are also present in the data in Figure 7, while other new peaks are also apparent under reaction condition. The absorption peaks around 1900 cm^{-1} can be assigned to gaseous NO and several overlapped peaks between 1700–1600 cm^{-1} can be assigned to the bent type adsorbed (NO^-) species, and so, NO adsorption is oxidative. From the

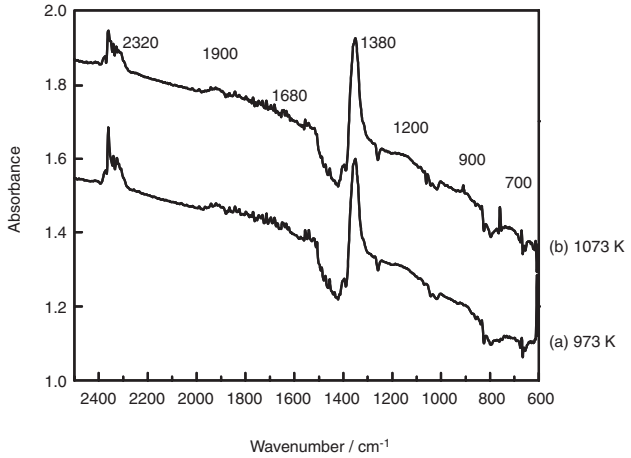

Figure 7. IR spectra of adsorbed NO on $Ba_{0.8}La_{0.2}Mn_{0.8}Mg_{0.2}O_3$ under NO decomposition conditions (NO adsorption: 773 K for 1 h at 10 kPa).

phase diagrams on $BaMnO_3$ oxide, Mn is a mixed-valence state of Mn^{III} and Mn^{IV} [36] and so bent NO may form by oxidation of Mn^{III}. This is reasonably considered because the crystal principally consists of Mn^{IV}, which is the formal valence number in this oxide. Strong absorption peaks and several weak peaks around 1380 cm^{-1} and also several broad absorption peaks around 1200 and 1000 cm^{-1} are also observed under these NO decomposition conditions. According to the values reported on a La_2O_3 catalyst,[35] the peaks at 1380, 1200, and 700 cm^{-1} can be assigned to the bridging or monodentate nitrate (NO_3^-) or nitrite (NO_2^-) species, or dimers such as $N_2O_2^{2-}$ and $N_2O_4^{2-}$. Therefore, under working conditions, the surface of the catalyst is covered with strongly adsorbed NO_x species and recovery of the active site is an important step for NO decomposition. This expectation is in good agreement with the first-order dependence of the rate on the NO partial pressure. It is also anticipated that the formation of NO_x species would be accelerated by the coexistence of oxygen in the gas feed. Therefore, the oxygen co-feed has a negative effect on NO decomposition. In addition, in Figure 7 absorption peaks around 2320 cm^{-1} are present that increase in intensity at the higher temperature. Although the absorption peaks of N_2O are close to that of CO_2 in the beam lines and some part is overlapped, these peaks could be assigned to adsorbed N_2O. Possibly N_2O is the intermediate species in NO decomposition.

Figure 8 shows the NO-TPD curves obtained after exposure to H_2 gas at 323 and 573 K for 30 min. As shown in Figure 8a, when the catalyst was exposed to H_2 at 323 K followed by adsorption of NO at 773 K, NO desorption was drastically decreased in comparison to the situation of no H_2 treatment (Figure 5). In particular, the amount of desorbed NO at lower temperatures radically decreased. In contrast, the amount of O_2 desorption and that of N_2 desorption at the higher temperatures is less affected by H_2 treatment at 323 K. However, H_2 treatment at 573 K, dramatically reduced the amount of O_2 and N_2, as well as NO desorption. Therefore, H_2 added to the reactants is quite effective for removing the surface NO_x species and recovering the active site for NO activation.

Figure 9 shows the effects of H_2 treatments on the adsorption state of NO as determined by IR measurements. In this experiment, after the NO was adsorbed, hydrogen at 10 kPa pressure was introduced and the sample was heated under circulating H_2 gas. In comparison with the simple evacuation treatment, the decrease in the absorbance due to nitrate species (NO_3^-) at 1330 cm^{-1} occurred at a much lower temperature,

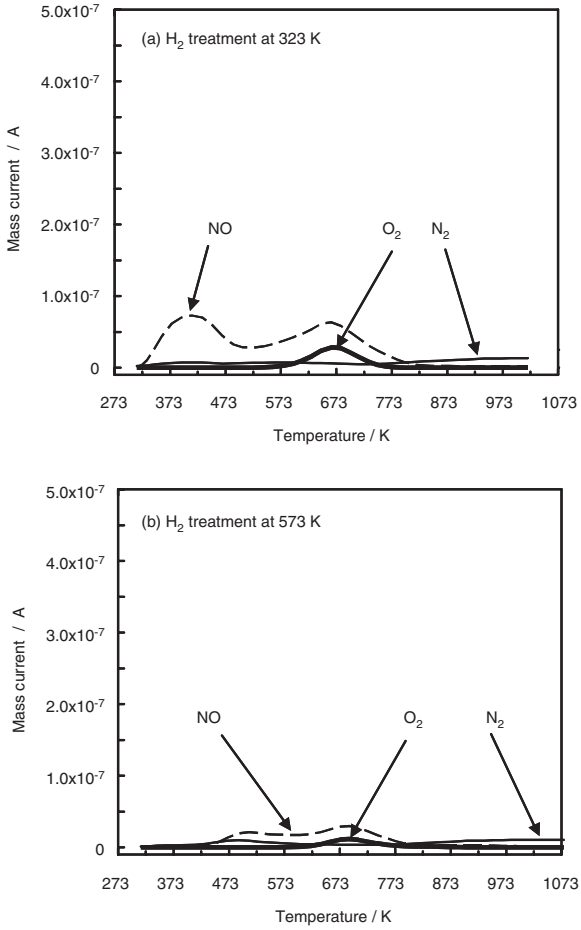

Figure 8. NO desorption profiles from $Ba_{0.8}La_{0.2}Mn_{0.8}Mg_{0.2}O_3$ after exposure to H_2 gas (NO adsorption: 773 K for 30 min).

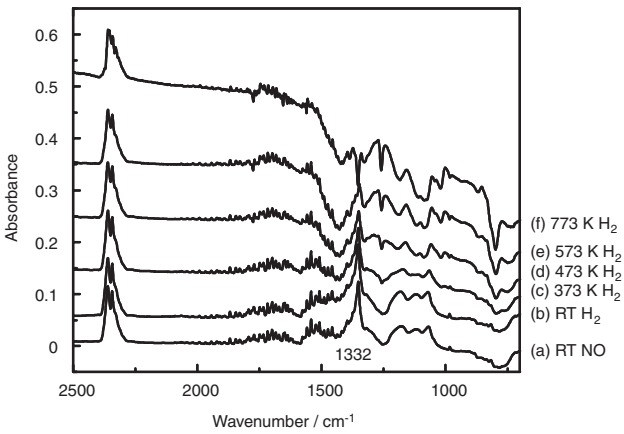

Figure 9. IR spectra of adsorbed NO on $Ba_{0.8}La_{0.2}Mn_{0.8}Mg_{0.2}O_3$ under circulating H_2 (NO adsorption: 773 K for 1 h, $P_{H_2} = 10$ kPa).

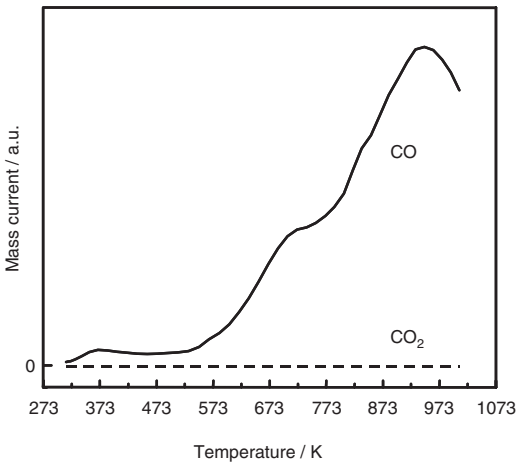

Figure 10. CO_2-TPD profile from $Ba_{0.8}La_{0.2}Mn_{0.8}Mg_{0.2}O_3$ (CO_2 adsorption: 773 K for 30 min).

and by 773 K, this peak had almost disappeared. Therefore, it is clear that the removal of surface NO_3^- species is highly accelerated by coexistence of H_2 in the gas phase and the main reason for the positive effects of added H_2.

Effects of Added CO_2 on the Adsorption State of NO. Since large negative effects of CO_2 co-feeding on the NO reaction are observed, the adsorption state of CO_2 on $Ba_{0.8}La_{0.2}Mn_{0.8}Mg_{0.2}O_3$ was also investigated (Figure 10). It is very interesting that the only desorption observed in the case of CO_2-TPD is that of CO, almost no CO_2 desorption being detected. In addition, the CO desorption occurred above 673 K and the desorption rate peaked at 973 K, which is a much higher temperature than that seen for NO or O_2. Therefore, adsorption of CO_2 on this catalyst is quite strong and dissociative, producing CO and oxygen adsorption species on the surface. The oxygen may also be strongly adsorbed on this catalyst and may block the active site of Ba(La)Mn(Mg)O_3 catalyst. Since the strongly adsorbed CO and O occupy the active site for NO decomposition, the NO decomposition activity is strongly suppressed by added CO_2. In order to confirm this hypothesis, the effect of CO_2 adsorption prior to NO-TPD was measured.

Figure 11 shows NO-TPD profiles for NO adsorbed at 773 K after exposure to CO_2 at 773 K for 30 min. Compared to the simple NO-TPD results (dashed line), it is obvious that the amount of NO desorption around 473 K drastically decreased after pretreatment with CO_2. In addition, CO desorption is also observed at temperatures higher than 773 K, similar to the NO-TPD signal. Furthermore, there is no desorption of N_2 observed at high temperatures (>873 K), as indicated by the mass signal for $m/e = 14$. These results suggest that CO_2 adsorption is stronger than that of NO, and the molecular and/or dissociatively adsorbed NO seems to be strongly inhibited by the presence of CO_2. As discussed in our previous study,[31] the NO decomposition activity of this Ba(La)-Mn(Mg)O_3 obeys a NO partial pressure dependence of P_{NO}.[1,19] Therefore, blocking of NO adsorption sites by CO_2 is the main reason for the negative effects of CO_2 co-feed. However, as was shown in Figure 4, addition of H_2 is effective for improving the NO decomposition activity. This could be also explained by the removal of surface oxygen and CO.

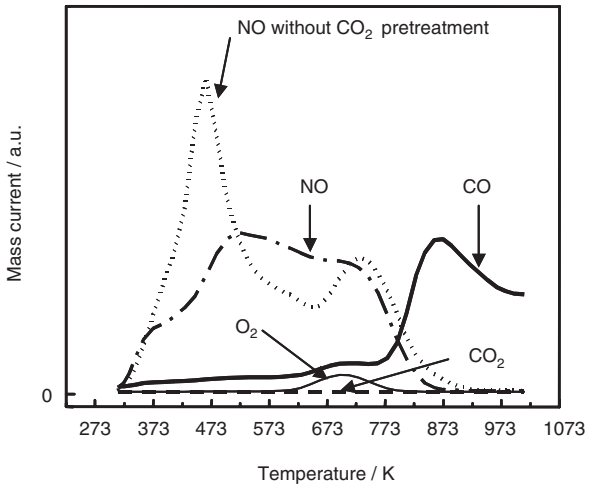

Figure 11. NO-TPD profile from $Ba_{0.8}La_{0.2}Mn_{0.8}Mg_{0.2}O_3$ after CO_2 pretreatment (CO_2 pretreatment: 773 K for 30 min, NO adsorption: 773 K for 30 min).

Therefore, at present, it is reasonable to suppose that the strong positive effects of co-feeding H_2 on NO decomposition in the presence of CO_2 are the removal of surface oxygen and/or CO.

CO_2 and H_2 Addition Effects on Reaction Steps. Considering the TPD and IR results, the following reaction steps and co-feeding gas effects are considered. In the initial step, NO adsorbs on the catalyst as bent NO, i.e. NO^-. Here, an electron may come from oxidation of Mn^{3+}, which is partially formed by mixed-valence state of Mn^{III} and Mn^{IV} or by electron transfer from oxide ion O^{2-} in the lattice. In accordance with the phase diagram, $BaMnO_3$ consists of Mn^{IV} and Mn^{III} under the reaction conditions.[36]

$$NO(gas) + e \rightarrow NO_{ad}^- \quad (1)$$

The second step seems to be a disproportionation reaction of NO to form NO_x surface species;

$$3NO_{ad}^- \rightarrow N_2 + (NO_3^-)_{ad} + 2e \text{ or } 2NO_{ad}^- \rightarrow 1/2N_2 + (NO_2^-)_{ad} + 2e \quad (2)$$

The surface nitrate or nitrosyl species (NO_x^- species) strongly block the active site and the removal of these NO_x species from the surface by reduction is the crucial step in the reaction. The existence of O_2 or CO_2 in the reactants, which form surface oxygen and/or carbon monoxide in the case of CO_2, accelerates the formation of surface NO_x^-, resulting in a negative effect on NO decomposition. In contrast, added H_2 is effective for the removal of such NO_3^- or NO_2^- to regenerate the active site and so the NO decomposition reaction was much improved by co-feeding of reductant H_2, particularly, at intermediate temperature. The following step is coupling of NO_x^- surface species as shown in the following step:

$$2(NO_3^-)_{ad} \rightarrow (N_2O_2)^{2-}{}_{ad} + O_2 \text{ or } 2(NO_3^-)_{ad} \rightarrow (N_2O_4)^{2-}{}_{ad} + 1/2O_2 \quad (3)$$

The desorption of O_2 occurs at a lower temperature than that of N_2 in NO-TPD profiles and this suggests the coupling of surface NO_x^- species to form O_2. Oxygen desorption occurring

from 723 K in NO-TPD suggests the coupling reaction occurs at temperatures where the NO decomposition reaction starts. The next step may be the formation of N_2O species, as suggested by the IR measurements.

$$(N_2O_2)_{ad}{}^{2-} \rightarrow N_2O^-{}_{ad} + 1/2O_2 + e \quad (4)$$

Since N_2O is easily decomposed on the catalyst to form N_2 and O_2 at higher temperatures, the final step of N_2O^- decomposition occurs quickly on this $BaMnO_3$-based oxide.

$$N_2O^-{}_{ad} \rightarrow N_2 + 1/2O_2 + e \quad (5)$$

A similar mechanism for NO decomposition has also been proposed for La_2O_3, Sr/La_2O_3, and $LaCo_{1-x}Cu_xO_3$.[24,33,34] A redox coupling of Mn between the oxidation states of +3 and +4 is an important step in this mechanism as reported in a previous paper,[29] the doped Mg seems to contribute by facilitating the Mn redox reaction by formation of oxygen vacancy and charge compensation.[31] The presence of an oxygen vacancy, which is reported to be the active site,[27,37] will be formed by doping Mg^{2+} with lower valence number than Mn and also, by charge compensation, Mn^{4+} becomes more stable and so removal of adsorbed oxygen or NO_x species becomes easier by improved redox cycle between Mn^{4+} and Mn^{3+}. Consequently, doping lower valence cations has prospective effects on the NO decomposition activity of $BaMnO_3$. In particular, ionic size of Mn^{II} (72 pm) is close to that of Mn^{3+} (64.5 pm) and Mn^{4+} (54.0 pm)[38] and so the most prospective effects are exhibited by doping Mg^{2+}.

Conclusion

This study investigated the effects of CO_2 on the NO decomposition activity of the perovskite oxide, $Ba_{0.8}La_{0.2}Mn_{0.8}Mg_{0.2}O_3$. The N_2 yield decreased with added CO_2 as ${P_{CO_2}}^{-0.32}$. The N_2 yield decreased from 70% to 30% on the addition of 1% CO_2, which is a much larger negative effect than that of O_2. The deleterious affect of CO_2 is not permanent and results from the inhibition of NO adsorption. By co-feeding H_2, the N_2 yield was greatly improved at temperatures near 773 K. This result suggests that the catalyst surface was covered by adsorbed oxygen or NO_x species and that the removal of surface oxygen or NO_x species that was formed by adsorption of NO might be the most important step for the NO decomposition reaction. Since the negative effects of CO_2 may arise from the strong adsorption of CO_2 on the active site for NO decomposition, CO_2 negative effects can be reduced by addition of H_2 as a reducing agent. The NO decomposition reaction seems to proceed through N_2O as a reaction intermediate. The surface of the catalyst was covered with bridging and monodentate nitrate species (NO_3^-) and the coupling reaction of NO_3^- seems to be the crucial step. Water is another inhibiter of NO decomposition. However, it is reported that the negative effects of water are not large in the case of $La_{0.7}Ba_{0.3}Mn_{0.8}In_{0.2}O_3$[30] because of high reaction temperature. Therefore, it is expected that the negative effects of water are also not large in this $BaMnO_3$ catalyst. Effects of H_2O addition on NO decomposition are now under investigation. Although a high reaction temperature is needed, the high N_2 yield suggests that the $BaMnO_3$-based perovskite oxide has a great potential as a NO removal catalyst.

References

1 M. Iwamoto, *Shokubai* **1995**, *37*, 614.
2 S. Kagawa, Y. Teraoka, *Hyomen* **1993**, *31*, 913.
3 H. Hamada, *Shokubai* **1991**, *33*, 320.
4 H. Hamada, Y. Kintaichi, M. Sasaki, T. Ito, M. Tabata, *Appl. Catal.* **1990**, *64*, L1.
5 S. Sato, Y. Yu-u, H. Yahiro, N. Mizuno, M. Iwamoto, *Appl. Catal.* **1991**, *70*, L1.
6 K. Yogo, M. Umeno, H. Watanabe, E. Kikuchi, *Catal. Lett.* **1993**, *19*, 131.
7 H. Hamada, Y. Kintaichi, M. Sasaki, T. Ito, T. Yoshinari, *Appl. Catal., A* **1992**, *88*, L1.
8 M. Iwamoto, H. Yahiro, H. K. Shin, M. Watanabe, J. Guo, M. Konno, T. Chikahisa, T. Murayama, *Appl. Catal., B* **1994**, *5*, L1.
9 K. Yogo, M. Ihara, I. Terasaki, E. Kikuchi, *Chem. Lett.* **1993**, 229.
10 Y. Li, J. N. Armor, *Appl. Catal., B* **1992**, *1*, L31.
11 Y. Nishizaka, M. Misono, *Chem. Lett.* **1993**, 1295.
12 A. Obuchi, A. Ohi, M. Nakamura, A. Ogata, K. Mizuno, H. Ohuchi, *Appl. Catal., B* **1993**, *2*, 71.
13 M. Inaba, Y. Kintaichi, H. Hamada, *Catal. Lett.* **1996**, *36*, 223.
14 H. Iwakuni, A. Takami, K. Komatsu, *Science and Technology in Catalysis 1998*, Elsevier, **1999**, p. 251.
15 M. Iwamoto, H. Yahiro, S. Shundo, Y. Yu-u, N. Mizuno, *Appl. Catal.* **1991**, *69*, L15.
16 W. Held, A. Koenig, T. Richter, L. Puppe, SAE Pap. **1990**, 900496.
17 H. Hamada, N. Matsubayashi, H. Shimada, Y. Kintaichi, T. Ito, A. Nishijima, *Catal. Lett.* **1990**, *5*, 189.
18 C. J. Bennett, P. S. Bennett, S. E. Golunski, J. W. Hayes, A. P. Walker, *Appl. Catal., A* **1992**, *86*, L1.
19 K. C. C. Kharas, *Appl. Catal., B* **1993**, *2*, 207.
20 H. Hamada, Y. Kintaichi, M. Sasaki, T. Ito, *Chem. Lett.* **1990**, 1069.
21 H. Yasuda, N. Mizuno, M. Misono, *J. Chem. Soc., Chem. Commun.* **1990**, 1094.
22 M. Iwamoto, H. Yahiro, K. Tanda, N. Mizuno, Y. Mine, S. Kagawa, *J. Phys. Chem.* **1991**, *95*, 3727.
23 Y. F. Chang, J. G. McCarty, *J. Catal.* **1998**, *178*, 408.
24 M. A. Vannice, A. B. Walters, X. J. Zhang, *J. Catal.* **1996**, *159*, 119.
25 S. Xie, M. P. Rosynek, J. H. Lunsford, *J. Catal.* **1999**, *188*, 24.
26 Y. Teraoka, H. Fukuda, S. Kagawa, *Chem. Lett.* **1990**, 1.
27 Y. Teraoka, T. Harada, S. Kagawa, *J. Chem. Soc., Faraday Trans.* **1998**, *94*, 1887.
28 J. Zhu, D. Xiao, J. Li, X. Xie, X. Yang, Y. Wu, *J. Mol. Catal. A: Chem.* **2005**, *233*, 29.
29 J. Zhu, D. Xiao, J. Li, X. Yang, Y. Wu, *J. Mol. Catal. A: Chem.* **2005**, *234*, 99.
30 T. Ishihara, M. Ando, K. Sada, K. Takiishi, K. Yamada, H. Nishiguchi, Y. Takita, *J. Catal.* **2003**, *220*, 104.
31 H. Iwakuni, Y. Shinmyou, H. Yano, H. Matsumoto, T. Ishihara, *Appl. Catal., B* **2007**, *74*, 299.
32 C. Tofan, D. Klvana, J. Kirchnerova, *Appl. Catal., B* **2002**, *36*, 311.
33 Z. Liu, J. Hao, L. Fu, T. Zhu, *Appl. Catal., B* **2003**, *44*, 355.
34 R. Spinicci, A. Delmastro, S. Ronchetti, A. Tofanari, *Mater. Chem. Phys.* **2003**, *78*, 393.

35 S. J. Huang, A. B. Walters, M. A. Vannice, *J. Catal.* **2000**, *192*, 29.
36 *Phase Equilibria Diagrams (Ver. 3.1.0)*, American Ceramic Society, **1971**, Vol. 3, Fig. 04176.
37 Z. Zhao, X. Yang, Y. Wu, *Appl. Catal., B* **1996**, *8*, 281.
38 R. D. Shannon, *Acta Crystallogr., Sect. A* **1976**, *32*, 751.